SAND2017-9267C

$Sc_xAl_{1-x}N$ Film Evaluation Using Contour Mode Resonators

Benjamin A. Griffin
Microsystems and Engineering Sciences Applications
Sandia National Laboratories
Albuquerque, United States
bagriff@sandia.gov

Michael D. Henry
Microsystems and Engineering Sciences Applications
Sandia National Laboratories
Albuquerque, United States

Robert W. Reger
Microsystems and Engineering Sciences Applications
Sandia National Laboratories
Albuquerque, United States

Bernd Heinz
Evatec AG
Trübbach, Switzerland
bernd.heinz@evatecnet.com

***Abstract*—Recent literature has focused on improving piezoelectric coupling coefficients by alloying aluminum nitride (AlN) with scandium (Sc). Akiyama et al. showed the highest piezoelectric coefficient increase of nearly four times for a 41% Sc substitution for Al. Thus far, studies mainly focus on material measurements such as x-ray diffraction or piezoelectric constants to assess the material quality. Although these measurements are useful to assess the improvement in the piezoelectric performance of the material, they do not address changes in the coupling coefficient and quality factor. Resonator structures are needed to directly extract these key performance parameters for film assessment. Fabrication integration, however, must be minimized to avoid obscuring film performance by extrinsic device effects. In this work, we assess a film evaluation tool using contour mode resonators (CMRs) to directly extract resonator performance for film comparison. Resonators formed from AlN, $Sc_{0.06}Al_{0.94}N$, and $Sc_{0.125}Al_{0.875}N$ films are compared to demonstrate the method.**

Keywords—scandium aluminum nitride, contour mode resonator, coupling coefficient, quality factor

I. Introduction

Aluminum nitride (AlN) piezoelectric resonators, specifically film bulk acoustic resonators (FBARs), dominate the current market for wireless radio frequency (RF) filters for cellular applications [1]. FBAR's success in comparison to other RF MEMS resonators is due to superior combination of bandwidth, out-of-band rejection, insertion loss, and complementary metal oxide semiconductor (CMOS) fabrication compatibility. A suspended piezoelectric film, along with top and bottom electrodes, as shown in Figure 1, forms an FBAR. When an alternating electric potential is applied across the piezoelectric film, it expands and contracts in the thickness direction. A resonance is formed through the thickness of the piezoelectric film when the thickness equals half a wavelength. Thus, film thickness sets an FBAR filter's center frequency. As a result, achieving even small frequency variations within a wafer requires the addition of multiple mask steps to manipulate film thickness over portions of the wafer.

Contour mode resonators (CMRs) overcome this limitation by achieving resonance in the plane of the film, where lithography establishes frequency rather than film thickness. Sandia's microresonator program has demonstrated this advantage with 32 kHz to 10 GHz resonators built in a single fabrication process [2]. A CMR example is shown in Figure 2, where a set of interdigitated fingers drive a resonance in the plane of the device. Because the frequency is set by the width of the resonating structure, frequencies are established by lithography rather than film thickness. This allows for a multitude of frequencies to be achieved in a single fabrication process and on a single chip.

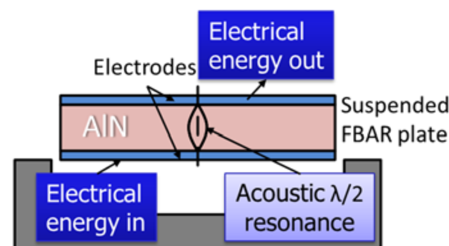

Figure 1 FBAR Resonator.

Although AlN CMRs have tremendous potential, they cannot meet the bandwidth requirements for many current RF needs because of the AlN's lower lateral coupling coefficient ($k_{31}^2 \sim 2\%$). The figure of merit (FOM) for resonators is the electromechanical coupling coefficient times the quality factor ($k^2 \cdot Q$). The FOM sets the lowest potential insertion loss of the resonator and has implications on filter bandwidth (BW). The minimum achievable bandwidth is set by the Q and the maximum BW by approximately half the coupling coefficient ($BW \sim \left(\frac{1}{2}\right) k^2$) [3]. The electromechanical coupling coefficient is a material dependent parameter which is a function of the piezoelectric film's permittivity, stiffness, and piezoelectric constants. Using material constants found in Table 1 and the stiffness matrix in [4], maximum material BW for AlN FBAR is approximately $k_{33}^2/2 = 3.1\%$.

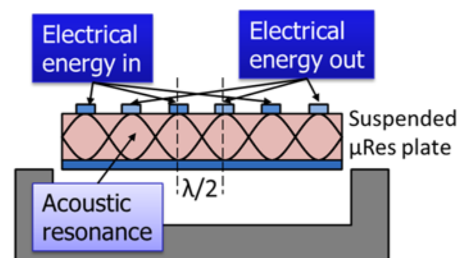

Figure 2 Contour mode resonator.

Table 1 Material properties of AlN and $Sc_{0.41}Al_{0.59}N$.

	d_{33} (pm/V)	d_{31} (pm/V)	c_{33}^E (GPa)	$1/s_{11}^E$ (GPa)	$\varepsilon_{33,r}$	k_{33}^2 (%)	k_{31}^2 (%)
AlN [4]	5.5	-2.6	395	283	11	6.3	2.0
$Sc_{0.41}Al_{0.59}N$ [5]	24	-13.5		227	16		29

Broader application of multi-frequency, CMR filters is constrained by the maximum bandwidth of the AlN lateral coupling coefficient. Using the material properties given in Table 1, the maximum CMR BW is approximately $k_{31}^2/2 \sim 1.0\%$. To widen potential application space for CMR resonators, innovation in nitride based piezoelectric films is needed to improve the lateral coupling coefficient.

Table 1 contains the material parameters extracted for a 41% Sc-alloying percentage. From these results, the lateral material coupling coefficient increases to 29%. A coupling coefficient of just 6% would allow revolutionary RF filter designs. Studies such as [5] mainly focus on material measurements such as x-ray diffraction or piezoelectric constants to assess the material quality. Although these measurements can be used to assess the improvement in the piezoelectric performance of the material, they do not address improvements in coupling coefficient and quality factor of resonators. The coupling coefficient is extracted via calculations combining multiple measurements. The quality factor cannot be measured from direct film measurements. Resonator structures are required to directly extract the key performance parameters for resonators.

Fabrication integration, however, can obscure film performance. For example, in [6], a CMR at 2.6 GHz with a coupling coefficient from 5.6% to 8.3% was developed, but the Q of 120 was limited by the electrode resistance. In addition, there was no AlN control film for direct comparison.

In this work, we assess a film evaluation tool using CMRs to directly extract resonator performance for film comparison. The top electrode only CMRs are formed using a two mask process to minimize integration effects. Arrays of resonator devices are formed to extract coupling coefficients as a function of frequency. An auto-prober is used to measure device arrays. This method allows direct comparisons between AlN and ScAlN films to compare coupling coefficients and quality factors to assess new films based off not only improvements in piezoelectric performance, but quality factor performance.

II. CMR Design

The CMR consists of two interlocking comb-shaped arrays of metallic electrodes integrated with a free-standing piezoelectric film membrane to form an interdigital transducer (IDT). Figure 3a show an example of a top view of an IDT CMR. Note that the finger spacing and aperture are controlled as a function of the designed wavelength. Figure 3b shows an example of a cross section perpendicular to the electrode fingers of an IDT CMR with electric field lines. The vertical component of the electric field formed between the input and output electrodes couples into lateral strain via the film's d_{31} piezoelectric coefficient. A standing symmetric Lamb wave is formed between the boundaries of the plate when the plate width is equal to an integer number of half-wavelengths. The electrodes are spaced center-to-center at half-wavelengths such

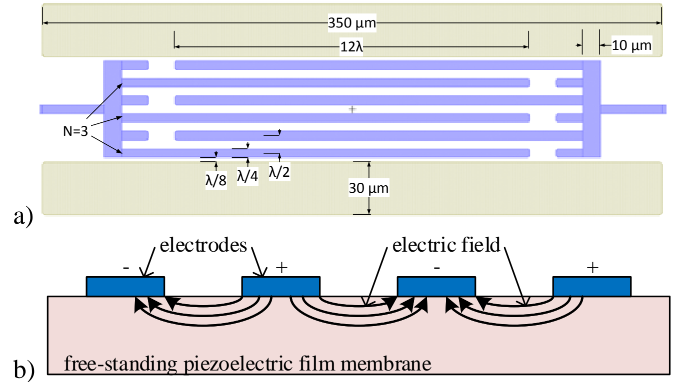

Figure 3 Freestanding IDT type CMR used for comparing FOM between films (a) Top down view of a 3 finger CMR showing the electrode and the release pit that defines the boundaries of the resonator. (b) Cross-section perpendicular to the electrodes of a 2-finger CMR of showing the electric field lines.

that they are centered on the points of maximum strain in the standing wave. The end electrodes are centered a quarter-wavelength from the end of the suspended membrane. The electrode widths are maintained at quarter-wavelength.

III. Resonator Fabrication

The resonator fabrication is kept as simple as possible to prevent integration affects from obscuring film comparisons. Figure 4 shows the fabrication steps used to form the IDT-type resonator. (a) First the piezoelectric film is deposited on a high resistivity ($10\ k\Omega \cdot$ cm) silicon (Si) substrate. Three films were assessed in this work: AlN, $Sc_{0.06}Al_{0.94}N$, and $Sc_{0.125}Al_{0.875}N$. The AlN and $Sc_{0.06}Al_{0.94}N$ films were deposited by pulsed direct current magnetron sputtering of metallic Al and $Al_{0.94}Sc_{0.06}$ targets in Ar + N_2 atmosphere at Evatec using a CLUSTERLINE® 200 II single wafer production tool. The $Sc_{0.125}Al_{0.875}N$ film was deposited by co-sputtering from Al and Sc targets in a multi-source MSQ200 module. All films were 0.75 µm thick. (b) Next, a 200 nm aluminum top electrode is

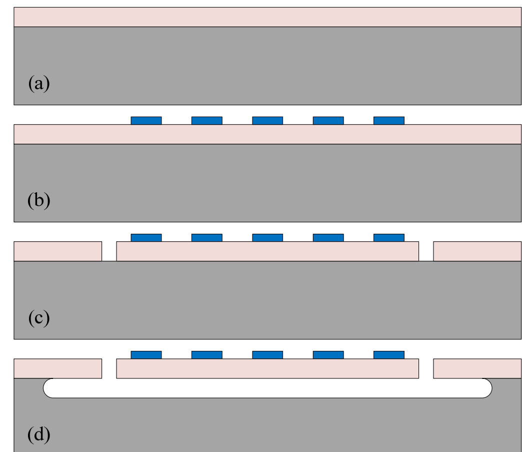

Figure 4 IDT CMR fabrication process showing (a) starting with piezoelectric film on silicon substrate (b) deposition and patterning of top electrode to form (c) piezoelectric film etch to the substrate (d) release via isotropic XeF_2 etch.

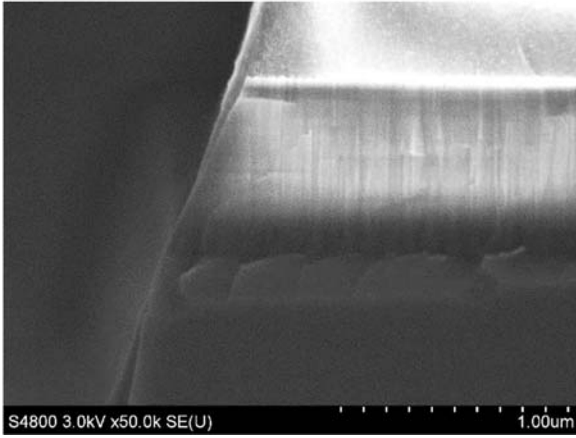

Figure 5 Cross sectional scanning electron micrograph of a $Sc_{0.06}Al_{0.94}N$ film on Si after etching.

deposited and patterned. The top electrode material selection is subject to choice as long as the sheet resistance is low enough to not load the quality factor, the electrode is compatible with release chemistry, and the electrode is consistent between the films under comparison. The thickness should be chosen to appropriately lower the sheet resistance without significantly altering the resonant mode. (c) The piezoelectric film is etched to define the resonator boundaries. This etch defines the wavelength of the resonator. A chlorine based etch is applied to etch both piezoelectric films. Due to the addition of Sc, the $Sc_{0.06}Al_{0.94}N$ and $Sc_{0.125}Al_{0.875}N$ films are noticeably more difficult to etch [7]. The scanning electron microscopy (SEM) image in Figure 5 shows a reasonably vertical sidewall profile for $Sc_{0.06}Al_{0.94}N$. (d) Finally, the CMR is suspended by isotropic etch of the Si using xenon difluoride (XeF_2). A microscope image of a completed CMR is shown in Figure 6.

Film Characterization

Rocking curve measurements demonstrated a full-width-half-maximum (FWHM) of 1.4° for both AlN and $Sc_{0.06}Al_{0.94}N$. The FWHM of the co-sputtered $Sc_{0.125}Al_{0.875}N$ film was 1.8°.

Resonator Characterization

An array of device wavelengths was designed to perform the material characterization. Wavelengths from 6-19 µm were fabricated. The device designs scaled with wavelength as shown in Figure 3a. Designs with three, four, and five finger pairs (defined as N in Figure 3a) were fabricated. An autoprober was used to probe devices across all wafers. An Agilent E5071C network analyzer collected s-parameters for each device. An example of S_{21} for four finger devices across the wafer is shown in Figure 7.

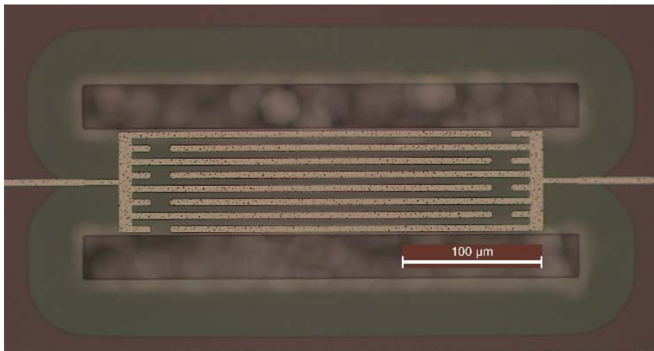

Figure 6 Top view of a four-finger fabricated CMR.

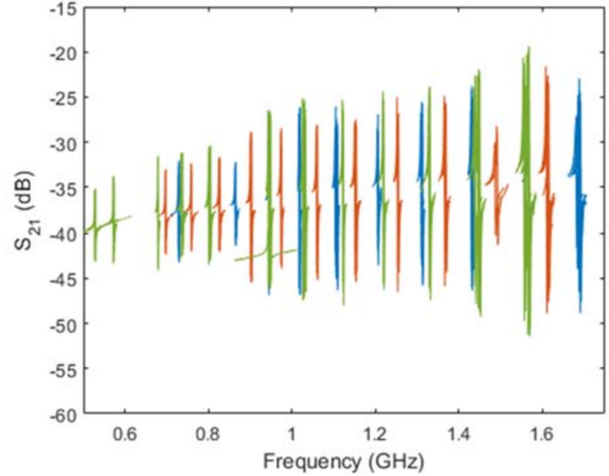

Figure 7 S_{21} for array of designs collected across wafer (AlN: blue, $Sc_{0.06}Al_{0.94}N$: red, $Sc_{0.125}Al_{0.875}N$: green).

From the S-parameters, quality factor and coupling coefficient are calculated. The quality factor (Q) is found by fitting the -3 dB bandwidth around the series resonance. The effective coupling coefficient is found using the series and parallel resonant frequencies, f_s and f_p, respectively, as

$$k_{eff}^2 = \frac{f_p^2 - f_s^2}{f_p^2} \tag{1}$$

Figure 8 shows a comparison of S_{21} measurements for resonators of a fixed wavelength for the three wafer types. As can be seen in the figure, the increasing Sc content lowers the resonant frequency of the device, indicating a lowering of the

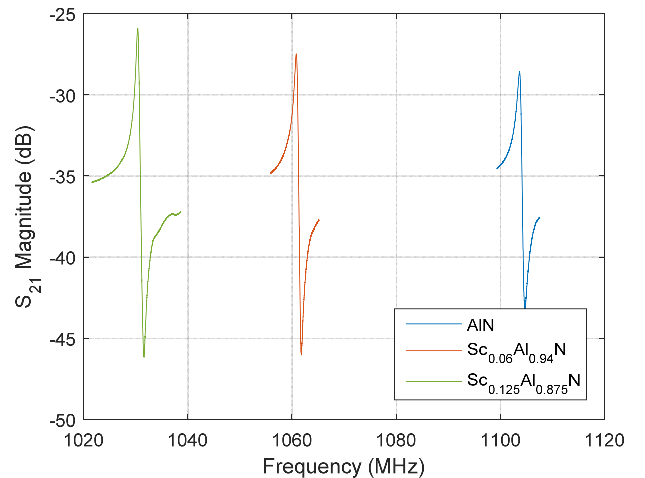

Figure 8 Comparison of S_{21} for a four-finger resonator with the same wavelength between AlN, $Sc_{0.06}Al_{0.94}N$, and $Sc_{0.125}Al_{0.875}N$ as a function of frequency.

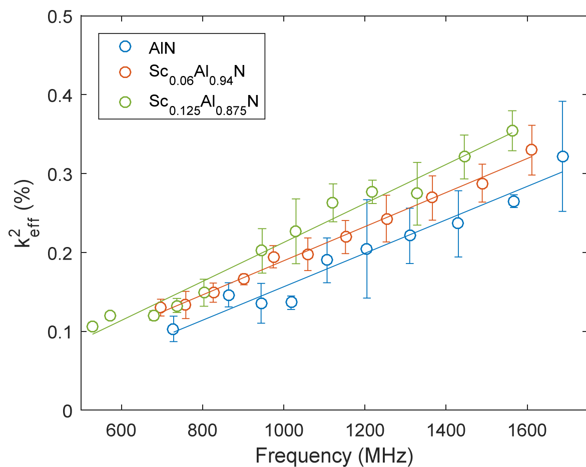

Figure 9 Comparison of the coupling coefficient between AlN (blue circles), $Sc_{0.06}Al_{0.94}N$ (red diamonds), and $Sc_{0.125}Al_{0.875}N$ (green triangles) as a function of frequency for four finger resonators.

speed of sound likely due to material softening due to the addition of Sc.

Figure 9 shows the coupling coefficient comparison between AlN, $Sc_{0.06}Al_{0.94}N$, and $Sc_{0.125}Al_{0.875}N$. Outliers were removed and considered a yield loss. Error bars represent two standard deviations. As expected, the $Sc_{0.06}Al_{0.94}N$ shows an increase in coupling coefficient in comparison to the AlN. The co-sputtered $Sc_{0.125}Al_{0.875}N$ also shows improvement over the $Sc_{0.06}Al_{0.94}N$. Future work will compare films of same Sc content via different deposition methods.

Figure 10 shows the quality factor comparison between AlN, $Sc_{0.06}Al_{0.94}N$, and $Sc_{0.125}Al_{0.875}N$. The quality factor varies over the wafer for a given wavelength likely due to process variability due to small lot volumes. Although the quality factor degrades for $Sc_{0.06}Al_{0.94}N$ in comparison to the AlN, it is recaptured for $Sc_{0.125}Al_{0.875}N$. Other works have also noted dependence of quality factor on Sc content [8]. Future work will investigate quality factor sensitivity to fabrication.

CONCLUSION

In this work, we presented a method to characterize piezoelectric thin films beyond x-ray diffraction and material characterization. Resonator coupling coefficient and quality factor were extracted via resonator fabrication and characterization. The resonator characterization showed a clear increase in coupling coefficient as expected with the addition of Sc to the AlN. However, a corresponding quality factor dependence on Sc content was also noted that would have been missed via conventional thin film characterization.

Demonstrating the value of this technique for film assessment, it required less than 48 hours from receipt of the films to perform the two-mask fabrication process, release the resonators, characterize them on an autoprober, and analyze the data. It is expected that a high volume, production facility could further optimize the turnaround time.

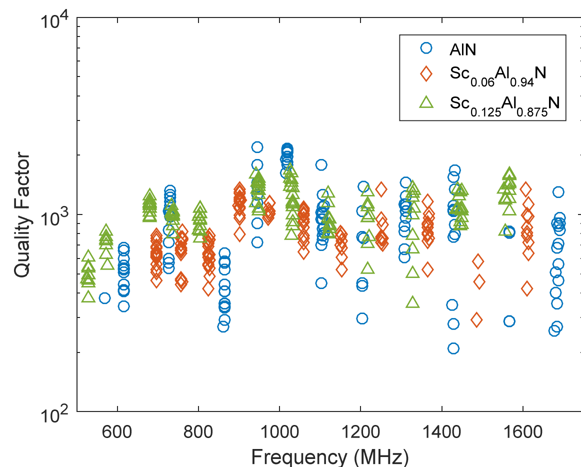

Figure 10 Comparison of the quality factor between AlN (blue circles), $Sc_{0.06}Al_{0.94}N$ (red diamonds), and $Sc_{0.125}Al_{0.875}N$ (green triangles) as a function of frequency.

ACKNOWLEDGMENT

This work was supported by the Laboratory Directed Research and Development (LDRD) program at Sandia National Laboratories. Sandia National Laboratories is a multimission laboratory managed and operated by National Technology and Engineering Solutions of Sandia LLC, a wholly owned subsidiary of Honeywell International Inc. for the U.S. Department of Energy's National Nuclear Security Administration under contract DE-NA0003525. The authors acknowledge fabrication support by the Sandia MESAFab operations team, especially T. Young and J. Mudrick, and test and measurement support by A. Schiess.

REFERENCES

[1] R. Ruby, "A Snapshot in Time: The Future in Filters for Cell Phones," *IEEE Microwave Magazine,* vol. 16, no. 7, pp. 46-59, 2015.

[2] B. A. Griffin, C. D. Nordquist, and M. D. Henry, "Beyond Aluminum Nitride: Piezoelectric Materials for RF MEMS Resonators," in *IEEE International Microwave Symposium*, Honolulu, Hawaii, 2017.

[3] C. D. Nordquist, R. H. Olsson, and J. G. Webster, "Radio Frequency Microelectromechanical Systems (RFMEMS)," in *Wiley Encyclopedia of Electrical and Electronics Engineering*: John Wiley & Sons, Inc., 1999.

[4] K. Tsubouchi and N. Mikoshiba, "Zero-Temperature-Coefficient SAW Devices on AlN Epitaxial Films," *IEEE Transactions on Sonics and Ultrasonics,* vol. 32, no. 5, pp. 634-644, 1985.

[5] M. Akiyama, K. Umeda, A. Honda, and T. Nagase, "Influence of scandium concentration on power generation figure of merit of scandium aluminum nitride thin films," *Applied Physics Letters,* vol. 102, Jan 2013, Art. no. 021915.

[6] A. Konno *et al.*, "ScAlN Lamb Wave Resonator in GHz Range Released by XeF2 Etching," *2013 IEEE International Ultrasonics Symposium,* pp. 1370-1373, 2013 2013.

[7] M. D. Henry, T. R. Young, and B. A. Griffin, "ScAlN Etch Mask for Highly Selective Silicon Etching," *Journal of Vacuum Science & Technology B,* vol. in press, 2017.

[8] M. A. Moreira, J. Bjurstrom, V. Yantchev, I. Katardjiev, and Iop, "Synthesis and characterization of highly c-textured Al(1-x)Sc(x)N thin films in view of telecom applications," in *Symposium M on More than Moore - Novel Materials Approaches for Functionalized Silicon Based Microelectronics at Spring Meeting of the European-Materials-Research-Society (E-MRS)*, Strasbourg, FRANCE, 2012, vol. 41, 2012.